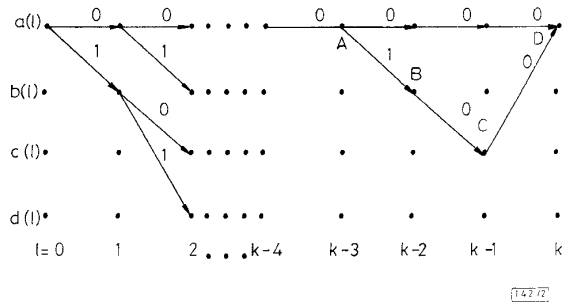

Fig. 2 *Modified trellis of uncoded 2PSK for improved sequence estimator*

$a(l)$: $\{\phi(l) = 0, \phi(l-1) = 0\}$, $b(l)$: $\{\phi(l) = 0, \phi(l-1) = 0\}$,
$c(l)$: $\{\phi(l) = 0, \phi(l-1) = \pi\}$, $d(l)$: $\{\phi(l) = 0, \phi(l-1) = \pi\}$
ABCD = shortest error event path

which differs from $\phi_0(k)$ only in the symbol $\phi_0(k-2)$. Because of the additional memory in the nodes, two paths which diverge from each other owing to the difference in a single transmitted symbol take more transitions before they remerge. For high SNR, the probability is very high that the sequence estimator only has to choose between $\phi_0(k)$ and $\phi_2(k)$ (and not a longer error event path) for the survivor at node $a(k)$, and in doing so it is deciding on the symbol $\phi(k-2)$. Using the same analysis as in the paragraph above, this decision is made by comparing

$$\mathrm{Re}\left[\left(\sum_{l=k-L,l\neq k-2} r(l)\right)^{*} r(k-2)\right]$$

against zero. Thus, the decision on $\phi(k-2)$ is made using the signal sample $r(k-2)$ with the aid of the reference

$$\tilde{v}(k) = \sum_{l=k-L,l\neq k-2} r(l)$$

which is a stronger reference for detecting $\phi(k-2)$ than the reference $v(k)$ is for detecting $\phi(k-1)$ in the original sequence estimator, because $\tilde{v}(k)$ has more signal samples closer to the $(k-2)$nd interval. On this basis, we expect the sequence estimator using the modified trellis to work better.

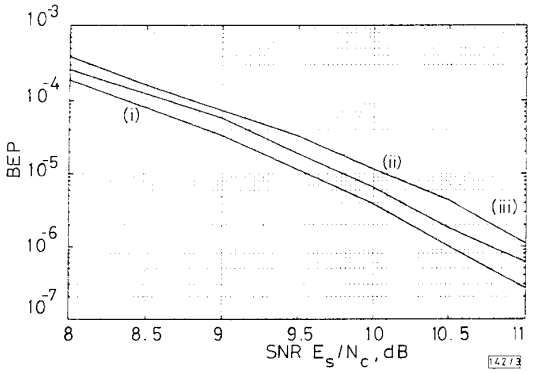

Fig. 3 *Simulated BEP of 2PSK, with sequence estimation in carrier phase noise*

(i) coherent (theoretical)–1/2 erfc$(E_s/N_0)^{1/2}$
(ii) sequence estimator of [1]
(iii) improved sequence estimator
$\sigma^2 = 0.02$ rad^2

We simulated the original sequence estimator of [1] and the improved estimator here for the case of 2PSK in the presence of a random-walk carrier phase model given by $\theta(k+1) = \theta(k) + w(k)$, where $\{w(k)\}$ is a sequence of independent, Gaussian random variables, each with mean zero and variance σ^2 (the phase noise variance). The simulated BEP results in Fig. 3 for $\sigma^2 = 0.02$ rad^2 with $L = 8$ symbol intervals show that the improved estimator here performs ~0.25dB better than the original estimator of [1] at BEPs of 10^{-5} to 10^{-6}.

Electronics Letters Online No: 19960850 *23 April 1996*

P.Y. Kam and F.H.K. Cheong (*Department of Electrical Engineering, National University of Singapore, 10 Kent Ridge Crescent, Singapore 119260, Republic of Singapore*)

References

1 POOY-YUEN KAM, and SINHA, P. : 'A Viterbi-type algorithm for efficient estimation of MPSK sequences over the Gaussian channel with unknown carrier phase', *IEEE Trans. Commun.*, 1995, **COM-43**, (9), pp. 2429–2433
2 KAM, P.Y.: 'Binary orthogonal signaling over the Gaussian channel with unknown phase/fading: new results and interpretations', *IEEE Trans. Commun.*, 1990, **COM-38**, (10), pp. 1686–1692
3 KAM, P.Y.: 'Maximum likelihood carrier phase recovery for linear suppressed-carrier digital data modulations', *IEEE Trans. Commun.*, 1986, **COM-34**, (6), pp. 522–527

Introducing time-frequency distribution with a 'complex-time' argument

S. Stanković and L. Stanković

Indexing terms: Signal processing, Time-frequency analysis

A distribution, highly concentrated along the instantaneous frequency, is introduced using a 'complex-time' signal argument. Realisation of a signal with complex argument, using a signal with a real argument, is presented.

Introduction: The high concentration of a distribution, along the instantaneous frequency, is one of the very important properties in time-frequency analysis [1]. Depending on the signal form, different distributions may be used successfully for that purpose [1 – 6]. For a signal of the form

$$x(t) = re^{j\phi(t)} \tag{1}$$

time-frequency presentations may be, generally, written as

$$TFD(t,\omega) = 2\pi r^{2q}\delta(\omega-\phi'(t))^{*}_{\omega} FT\{e^{jQ(t,\tau)}\}^{*}_{\omega} W(\omega) \tag{2}$$

where $Q(t, \tau)$ is a factor defining distribution spread around the instantaneous frequency, $W(\omega)$ is the window's Fourier transform, and q is a constant. In the case of an ideally concentrated distribution, factor $Q(t, \tau)$ should be equal to zero. This may be achieved only by the specific distributions for special signal forms [1, 4, 5]. Spread factor $Q(t, \tau)$ is presented in Table 1 for some interesting distributions (from the point of high concentration) [1, 4 – 6] obtained using a Taylor series expansion of the phase function. Results from Table 1 are illustrated in Figs. 1 and 2, for signals $x(t) = e^{j(50t^3-130t)}$ and $x(t) = e^{j(-10t^5+50t^3-130t)}$, respectively. It may be observed that in both cases the L-Wigner distribution (with L=2) [5, 6] reduces artifacts better than the Wigner distribution. Further improvement of this distribution may be achieved by increasing the distribution order L. Polynomial Wigner distribution [4] produces complete concentration at the instantaneous frequency in the first case, while it is very sensitive to the fifth order term in the second case (in this case a higher order polynomial Wigner distribution should be used, [4]).

'Complex-time' distribution: A significant decreasing of spread flinction $Q(t, \tau)$ (meaning the concentration improvement), may be achieved by defining a distribution with a 'complex-time' argument:

$$CTD(t,\omega) = \int_{-\infty}^{\infty} x\left(t+\frac{\tau}{4}\right)x^{*}\left(t-\frac{\tau}{4}\right)x^{-j}\left(t+j\frac{\tau}{4}\right)x^{j}\left(t-j\frac{\tau}{4}\right)e^{-j\omega\tau}d\tau \tag{3}$$

Factor $Q(t, \tau)$, for this distribution is

$$Q(t,\tau)=\phi^{(5)}(t)\frac{\tau^5}{4^45!}+\phi^{(9)}(t)\frac{\tau^9}{4^89!}+\phi^{(13)}(t)\frac{\tau^{13}}{4^{12}13!}\cdots \quad (4)$$

Table 1: Spread factor in some time-frequency distributions

	Distribution
Spectrogram	$SPEC(t,\omega)=\left\|\int_{-\infty}^{\infty}w(\tau)x(t+\tau)e^{-j\omega\tau}d\tau\right\|^2$
Wigner distribution	$WD(t,\omega)=\int_{-\infty}^{\infty}w(\tau)x(t+\frac{\tau}{2})x^*(t-\frac{\tau}{2})e^{-j\omega t}d\tau$
L-Wigner distribution	$LWD(t,\omega)=\int_{-\infty}^{\infty}w(\tau)x^L(t+\frac{\tau}{2L})x^{*L}(t-\frac{\tau}{2L})e^{-j\omega t}d\tau$
Fourth order polynomial Wigner distribution	$PWVD(t,\omega)=\int_{-\infty}^{\infty}w(\tau)x^2(t+0.675\tau)x^{*2}(t-0.675\tau)$ $x^*(t+0.85\tau)x(t-0.85\tau)e^{-j\omega t}d\tau$
	Spread factor
Spectrogram	$Q(t,\tau)=\phi^{(2)}(t)\frac{\tau^2}{2!}+\phi^{(3)}(t)\frac{\tau^3}{3!}+\phi^{(4)}(t)\frac{\tau^4}{2!}+\cdots$
Wigner distribution	$Q(t,\tau)=\phi^{(3)}(t)\frac{\tau^3}{2^23!}+\phi^{(5)}(t)\frac{\tau^5}{2^45!}+\phi^{(7)}(t)\frac{\tau^7}{2^67!}\cdots$
L-Wigner distribution	$Q(t,\tau)=\phi^{(3)}(t)\frac{\tau^3}{2^23!L^2}+\phi^{(5)}(t)\frac{\tau^5}{2^45!L^4}+\phi^{(7)}(t)\frac{\tau^7}{2^67!L^6}\cdots$
Fourth order polynomial Wigner distribution	$Q(t,\tau)=-0.327\frac{\phi^{5}(t)}{5!}\tau^5-0.386\frac{\phi^{(7)}(t)}{7!}\tau^7+\cdots$

The dominant (first) term in the expansion of $Q(t, \tau)$ is of the fifth order. All terms are significantly reduced with respect to these in the Wigner distribution (e.g. the third order term does not exist; the coefficient with the fifth order term is reduced 2^4 times; the seventh term does not exist; the coefficient with the ninth order term is reduced 2^8 times etc.). In the 'complex-time' distribution,

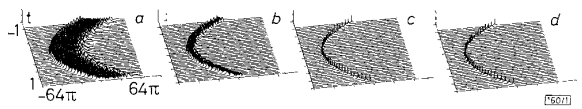

Fig. 1 *Time-frequency representation of signal with polynomial phase of the third order*

a Wigner distribution, *b* L-Wigner distribution, *c* Polynomial Wigner distribution, *d* 'Complex-time' distribution

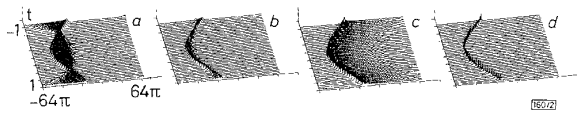

Fig. 2 *Time-frequency representation of signal with polynomial phase of the fifth order*

a Wigner distribution, *b* L-Wigner distribution, *c* Polynomial Wigner distribution, *d* 'Complex-time' distribution

the number of terms in $Q(t, \tau)$ is two times smaller than in the Wigner distribution, since the seventh, ninth, 11th etc. terms are completely eliminated. Illustration of this distribution is presented in Fig. 1*c* and Fig. 2*c*. In both cases the distribution is completely, or almost completely, concentrated at the instantaneous frequency. Note that the 'complex-time' distribution also satisfies some very important properties for the time-frequency signal analysis:

(i) 'Complex-time' distribution is always real for signals of the form in eqn. 1.

(ii) 'Complex-time' distribution satisfies the time marginal condition for any signal

$$\frac{1}{2\pi}\int_{\omega}CDT(t,\omega)d\omega=|x(t)|^2$$

(iii) The unbiased energy condition is satisfied for any signal

$$\frac{1}{2\pi}\int_t\int_{\omega}CDT(t,\omega)dtd\omega=\int_t|x(t)|^2dt=E_x$$

(iv) The frequency marginal is satisfied under the condition that the factor of $Q(t, \tau)$ may be neglected.

(v) If CTD(t,ω) is a distribution of signal $x(t)$, then CTD(t–T,ω) is the distribution of signal $x(t–T)$.

(vi) If signal $x(t)$ is time limited to an interval $|t| \leq T$, then CTD(t,ω) is also limited to the same time interval.

(vii) If CTD(t,ω) is a distribution of $x(t)$, then CTD(t,ω–ω$_0$) is a distribution of signal $x(t)e^{j\omega_0 t}$.

(viii) The 'complex time' distribution of the scaled signal $\sqrt{|a|}x(at)$ is CTD(at,ω/a).

Numerical realisation - analytic extension of a signal: For numerical realisation, a discrete version of the 'complex-time' distribution has to be defined. According to the analogue definition in eqn. 3, discrete pseudo form is given by

$$CTD(n,k)=\sum_{-N/2+1}^{N/2}w(m)x(n+m)x^*(n-m)\times x^{-j}(n+jm)x^j(n-jm)e^{-j\frac{2\pi}{N}4mk} \quad (5)$$

where $w(m)$ is a window. The signal has to be oversampled twice with respect to the sampling interval in the Wigner distribution. Theoretically, realisation of the CTD is very simple, according to the definition in eqn. 5. It is a DFT of $w(m)x(n+m)x^*(n–m)$ $x^{-j}(n+jm)x^j(n–jm)$. But, in practical realisations, the values of $x(n)$ are available only along the real axis, The values with complex argument $x(n+jm)$ are not known and they must be determined from the values on the real-time axis. Here, we will present a way of getting a signal with the 'complex-time' argument, based on the real-time-argument signal. This problem is mathematically well studied and known as an analytical extension of the real argument function. Let us begin from the Fourier transform pair:

$$x(n)=\frac{1}{N}\sum_{k=-N/2}^{N/2-1}X(k)e^{j\frac{2\pi}{N}nk}$$
$$X(k)=\frac{1}{N}\sum_{k=-N/2}^{N/2-1}x(n)e^{-j\frac{2\pi}{N}nk} \quad (6)$$

where N is an even number. It is known that the analytical extension of function e^{jan} is given by e^{jaz} where $z = n+jm$ is a complex argument. The previous analytical extension is valid for $|z| < \infty$. Consequently, the analytic extension of signal $x(n)$ is defined as a sum of the analytic extensions of complex exponential functions, and it is given by:

$$x(n+jm)=\frac{1}{N}\sum_{k=-N/2}^{N}X(k)e^{-\frac{2\pi}{N}mk}e^{j\frac{2\pi}{N}nk} \quad (7)$$

with a region of convergence $|n+jm| < \infty$ for $N < \infty$. This expression may now be used for a very efficient numerical realisation: if we multiply $X(k)$ = FFT[$x(n)$] by exp(–2πmk/N), for a given m, then $x(n+jm)$ is obtained as $x(n+jm)$ = IFFT[$X(k)$exp(–2πmk/N)]. This is the method we used in numerical examples. Eqn. 7 may be transformed in the following way: since $X(k)$ is the Fourier transform of signal $x(n)$, eqn. 7 becomes

$$x(n+jm)=\frac{1}{N}\sum_{l=-m}^{M-1}x(l)e^{(j(n-l)-m)\frac{\pi}{N}}\frac{\sinh[(j(n-l)-m)\pi]}{\sinh[(j(n-l)-m)\frac{\pi}{N}]} \quad \text{for } 2M=N \quad (8)$$

This way, the signal with a complex argument is obtained from the one with the real argument. Note that for $m = 0$, the very well known form of the sampling theorem of periodic signals is obtained.

Numerical example: An illustration of the above relations will be given on the time-frequency representation of the signal:

$$x(t)=e^{j(a_1\cos(b_1t)+a_2\cos(b_2t))} \quad (9)$$

where $a_1 = 3$; $b_1 = \pi$; $a_2 = 1/3$; $b_2 = 3\pi$. Discrete values of $x(n)$ are obtained by sampling signal $x(t)$ with a sampling period $\Delta t = 2/N$,

$N = 64$. Interval $-1 \le t \le 1$ is considered. A window $\exp(-(4\tau)^{10})$, close to a rectangular one, is used for $|\tau| < 1/2$. The realisation is carried out according to eqn. 7 and using the FFT algorithms. Fig. 3 completely confirms our previous conclusions on the distribution concentration. In the numerical realisation, we should carefully use the above relations in the computation of a signal with a complex argument, since for large values of argument m (which is limited by window $w(m)$ width, eqn. 5) we may find ourselves outside the computer (program) computation precision, which would cause an error. If we want to use very wide windows $w(m)$, and very large m, an extended precision may be needed.

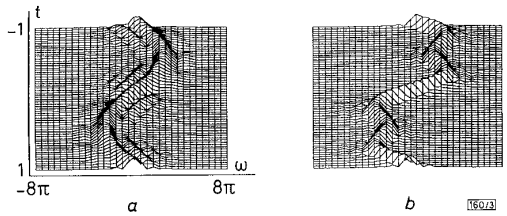

Fig. 3 *Time-frequency representation of discrete signal*

a Wigner distribution, *b* 'Complex-time' distribution obtained using an analytic extension of the signal

Conclusion: The 'complex-time' distribution is proposed and analysed. It has been shown that the artifacts induced by this distribution are significantly reduced with respect to all other known distributions.

24 April 1996
Electronics Letters Online No: 19960849

S. Stanković and L. Stanković (*Elektrotechnicki fakultet, University of Montenegro, Podgorica, Montenegro, Yugoslavia*)

References

1 COHEN, L.: 'Distributions concentrated along the instantaneous frequency'. SPIE, Adv. Signal Process. Algorithm Archit. and Implement., 1990, **1348**, pp. 149–157
2 HLAWATSCH, F., and BOUDREAUX-BARTELS, G.F.: 'Linear and quadratic time-frequency signal representations', *IEEE Signal Process. Mag.*, 1992, **9**, (2), pp. 21–67
3 STANKOVIĆ, L.J.: 'An analysis of some time-frequency and time-scale distributions', *Annales des Telecomunications*, 1994, **49**, (9/10), pp. 505–517
4 BOASHASH, B., and O'SHEA, P.: 'Polynomial Wigner-Ville distributions and their relationship to time-varying higher order spectra', *IEEE Trans. Sig. Process.*, 1994, **SP-42**, (1), pp. 216–220
5 STANKOVIĆ, L.J., and STANKOVIĆ, S.: 'An analysis of the instantaneous frequency representation by some time-frequency distributions - Generalised Wigner distribution', *IEEE Trans. Signal Process.*, 1995, **SP-43**, (2), pp. 549–552
6 STANKOVIĆ, L.J.: 'A multitime definition of the Wigner higher order distribution: L-Wigner distribution', *IEEE Signal Process. Lett.*, 1994, **1**, (7), pp. 106–109

Tomlinson-Harashima precoding for the magnetic recording channel

D. Krueger and J.R. Cruz

Indexing terms: Magnetic recording, Decision feedback equalisers

A new view on Tomlinson-Harashima (TH) precoding demonstrates the applicability of this precoding technique to input restricted channels. TH precoders of this kind are derived, and a hybrid of decision feedback equalisation and TH precoding is proposed.

To obtain equalisation without noise enhancement or error propagation, the input signal may be passed through an inverse channel filter prior to transmission. However, it is often impossible or impractical to invert the channel response. In this case the addition of a modulo element as shown in Fig. 1 may be made. The function of this element is to map a real input into the range $[-M, M)$ by adding some multiple of $2M$. Thus, if $c(D) = \text{round}(a(D)/2M)$ for some input sequence $a(D)$, the corresponding output sequence will be $b(D) = a(D) - 2Mc(D)$. This technique is known as Tomlinson-Harashima (TH) precoding [1, 2], and it produces the following noiseless channel output:

$$x(D) = v(D) - 2Mc(D) \tag{1}$$

As long as the input sequence $v(D)$ is contained within some interval of sise $2M$ (centred at r), it can be uniquely determined from the noiseless output using a modulo element as shown in Fig. 2. A value for M is chosen using the range of the input and the distance δ between constellation points:

$$2M = \max(v) - \min(v) + \delta \tag{2}$$

TH precoding as implemented in Fig. 1 cannot generally be used in the magnetic saturation recording channel because $w(D)$ does not satisfy the constraint that the write current be ±1 only.

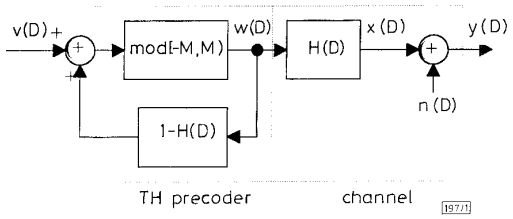

Fig. 1 *Block diagram of TH precoding technique*

Example 1: Assume the magnetic recording channel is equalised to $H(D) = 1-D$. Working from the constraints set on $w(D)$, use of eqn. 2 yields $M = 2$. If bipolar signals are used for $v(D)$, the necessary signals for $w(D)$ are elements of the set $\{-2, -1, 0, +1\}$, which does not satisfy the channel input constraints.

With suitable modifications, inverse filtering or TH precoding may still be used when the channel has input constraints. Recall that the input to the precoder corresponds to the desired output (modulo $2M$). The reason the previous example failed is that the bipolar signals chosen for $v(D)$ do not correspond to channel outputs consistent with the input constraints.

Example 2: The output of the magnetic recording channel equalised to $H(D) = 1-D$ is composed of elements from the set $\{-2, 0, +2\}$. Choosing the elements of $v(D)$ to be $\{0, 2\}$ allows the necessary signals for $w(D)$ to be the set $\{-1, +1\}$.

Close examination of Example 2 reveals it to be equivalent to the traditional form of precoding for magnetic recording, where a nonzero input to the precoder causes a sign change at the precoder output and a zero input causes no change. These inputs translate at the channel output into a peak and absence thereof, respectively. This example can be generalised to provide a precoding method for all similarly constrained partial response channels.

Example 3: Let the magnetic recording channel be equalised to

$$H(D) = \sum_{k=0}^{L} h_k D^k \tag{3}$$

where $h_0 = 1$ and $h_k \in \mathbf{Z}$ (the set of integers). When $w(D)$ is constrained to ±1, the noiseless channel output will be a subset of $2\mathbf{Z}$ (when the sum of h_k is even) or it will be a subset of $2\mathbf{Z}+1$ (when the sum of h_k is odd). In both cases the possible channel outputs can be partitioned into two sets. In the first case, the outputs can be split into the set of integers congruent modulo 4 to 0, and the set of integers congruent modulo 4 to 2. Outputs from this first set will be produced whenever the precoder input is 0, and outputs from the second set whenever the precoder input is 2. Thus choosing the signal constellation of $v(D)$ to be $\{0, 2\}$ permits the use of precoding on these input constrained channels. In the second case, the outputs can be split into the set of integers congruent modulo 4 to –1, and the set of integers congruent modulo 4 to +1. Channel outputs from the first set will result whenever the precoder input is –1, and outputs from the second set will result whenever the precoder input is +1. Thus choosing the signal constellation of $v(D)$ to be $\{-1, +1\}$ permits the use of precoding on these input constrained channels.